Title	非相溶ポリプロピレンブレンドが示す流動誘起結晶化挙動とレオロジー特性
Author(s)	北畠, 志温
Citation	
Issue Date	2025-03
Type	Thesis or Dissertation
Text version	none
URL	http://hdl.handle.net/10119/19852
Rights	
Description	Supervisor: 山口 政之, 先端科学技術研究科, 修士 (マテリアルサイエンス)

Effect of the addition of an immiscible polymer on the flow-induced crystallization of polypropylene

Shion Kitabatake (Yamaguchi Masayuki Lab.)

Introduction

Owing to its importance during plastic product, flow-induced crystallization has been actively studied for a long time [1][2]. One of the critical conditions for flow-induced crystallization is expressed by the Rouse–Weissenberg number Wi_R, which should be larger than 1 (eqution (1)). Furthermore, the Rouse time τ_R is proportional to the square of the molecular weight M, which is often expressed using the average molecular weight between entanglement couplings, i.e., M_e, as denoted in equation (2):

$$Wi_R \equiv \dot{\gamma}\tau_R > 1 \qquad (1)$$

$$\tau_R = \tau_e \left(M / M_e \right)^2 \qquad (2)$$

where τ_e is the Rouse time of an entanglement strand. For isotactic polypropylene (PP), the τ_e is 1.5×10^{-7} s at 170 °C [3] and the M_e is 5250 [4].

For immiscible polymer blends, the viscosity ratio plays an important role in the deformation of each phase flow. When the viscosity of a dispersed phase is higher than that of a continuous phase under shear flow, the situation is similar to that in a filler-dispersed system. Under this condition, the critical capillary number becomes infinity [5].

In the high-temperature region beyond the melting point of PP, the dispersed polymethylmethacrylate (PMMA) droplets deform affinely along with the PP when PMMA has low molecular weight. Viscosity of these prolonged PMMA dispersions promptly increases near the glass transition temperature of PMMA prior to PP crystallization, during cooling. As a result, the PMMA dispersions are hardly deformed under shear flow. Because this situation increases the shear rate increase of the matrix, it should promote shear-induced crystallization of PP. Under elongational flow, they enhance the drawdown force, i.e., the force required to stretch an extruded strand uniaxially, by the same mechanism, which was theoretically explained in the literature [6-8].

Herein, I studied immiscible PP/PMMA blends, Focusing on the effect of shear flow on shear-induced crystallization under non-isothermal conditions.

Experimental

(1) Sample preparation

PP and Three types of PMMA with different molecular weights, indicated as PMMA-L, PMMA-M, and PMMA-H were used. The weight-avarage molecular weights were 3.7×10^5 for PP, and 7.4×10^3 for PMMA-L, 8.9×10^4 for PMMA-M, and 1.9×10^5 for PMMA-H respectively. The samples of PP and PP/PMMA (70/30) blends were prepared using an internal mixer (Labo Plastmill 10M100; Toyo Seiki Seisaku-sho, Tokyo, Japan) at a blade rotation speed of 30 rpm at 190 ^{o}C for 3 min. The weight fraction of PMMA in the blends was 30 wt%, and tris[(2,4-di-tert-buthylphenyl)phosphate] (Irganox1010; Ciba, Bazel, Switzerland) and pentaerythritol tetrakis[3-(3,5-di-tert-buthyl-4-hydroxyphenyl)propionate] (Irgafos168; Ciba) were added as thermal stabilizers. Then the mixed samples were compressed into flat films at 190 ^{o}C and 20 MPa for 3 min, then quenched at 30 ^{o}C and 10 MPa for 3 min. Each film was cut and used to evaluate its rheological properties.

(2) Measurements

A cone-and-plate rheometer (TR-2000ex; TA instruments, New Castles, USA) was used to evaluate the frequency dependence of oscillatory shear moduli such as storage modulus G' and loss modulus G''. The measurements were performed at various temperatures. The cone angle was 4^{o} and its diameter was 25 mm. Furthermore, the rheometer was also used to evaluate the steady-state shear stress and primary normal stress difference at 190 ^{o}C.

The crystallization behavior with/without shear history was evaluated using a parallel-plate shear-stage made of quartz (CSS450; Linkam Scientific Instruments, Surrey, UK), which was set in a polarizing optical microscope (POM) operating in a crossed polar configuration (Leica DM2700P; Leica Microsystems, Wetzlar, Germany) equipped with the shear-stage covered in a temperature-controlled chamber. A round window with a diameter of 2.8 mm was located at 7.5 mm from the center of the plate. After adjusting the gap to 100 μm at 190 ^{o}C, the sample was quenched to 80 ^{o}C for the focus adjustment of a POM. Then it was heated at 190 ^{o}C for 5 min to melt crystals. The sample was quenched from 190 to 160 ^{o}C at a constant cooling rate of 30 ^{o}C min^{-1} and various shear rates. The depolarized light intensity (DLI), measured by a photo detector (PM16-121; Thorlabs, Newton, MA, USA) through a band-pass filter of 633 nm, was calculated using the following equation (3);

$$DLI(\%) = \frac{I_0 - I_X}{I_{//} - I_X} \times 100 \tag{3}$$

where I_X and $I_{//}$ are the light intensities without a sample under crossed and parallel polars respectively. I_0 is the light intensity passing through a sample under crossed polars. In this study, we used white light was used as a light source. After measurements, the sample was removed from the plates.

The orientation of PP chain was evaluated using a two-dimension wide-angle X-ray diffraction (2D-WAXD) by an XRD machine (SmartLab; Rigaku, Akishima, Japan). The sample was exposed to the graphite-monochromatized Cu Kα X-ray beam at 45 KV and 200 mA for 3min.

Morphology of compression-molded films after shear history was observed using a scanning electron microscope (SEM) (S-4100; Hitachi, Tokyo, Japan). After the films were cut using a microtome (RX-860; Yamato Kohki, Asaka, Japan) with spraying with liquid nitrogen, the cut surface of the film was then immersed in acetone for PP/PMMA for 1 day to remove the dispersions. Subsequently, the samples were dried for 5 hours to remove the solvent before sputter-coating with Pt-Pd.

Results and discussion

The rheological properties of three types of PMMA were evaluated. Fig. 1 shows the master curves of angular frequency ω dependence of shear storage modulus G' and loss modulus G'' at the reference temperature T_{r} of 190 °C. The measurements were performed at various temperatures from 110 to 190 °C. As shown in Fig. 1, the rubbery and flow regions were detected from high to low angular frequency for PMMA-M and PMMA-H. In contrast, PMMA-L showed the transition and flow regions without the rubbery region. This was as expected because the average molecular weight of PMMA-L was lower than its entanglement molecular weight M_e (13600) [4].

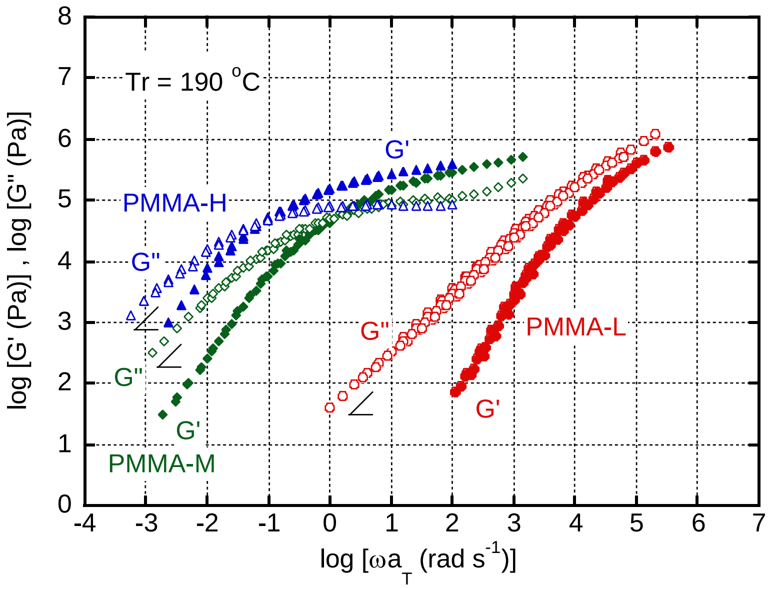

Fig. 1. Master curves of angular frequency dependence of (closed symbols) shear storage modulus G' and (open symbols) loss modulus G'' for (circles) PMMA-L, (diamonds) PMMA-M, and (triangles) PMMA-H at the reference temperature T_r of 190 °C.

Fig. 2 shows SEM images of the cut surface of the compression-molded films. The blend sample was observed after removal of PMMA by acetone. The dark spherical areas represent the PMMA dispersion. As seen in the images, the phase-separated structure, i.e., sea-island structure, was clearly detected. The average sizes and their standard deviations were 7.2 μm (4.5 μm) for PP/PMMA-L, 11.0 μm (7.5 μm) for PP/PMMA-M, and 12.3 μm (8.7 μm) for PP/PMMA-H.

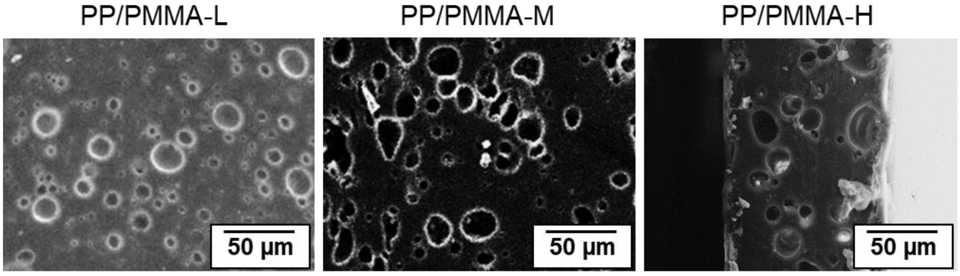

Fig. 2. SEM images of the cut surfaces of the compression-molded films.

Fig. 3 shows the crystallization behavior of the depolarized light intensity (DLI), i.e., transmitted light intensity through crossed polars and a color filter at cooling process. The samples were exposed to shear from 190 to 160 ^{o}C at shear rates of 1, 10, 30, and 50 s^{-1}. The DLI values increased around at 115 ^{o}C for PP and blend samples without shear. However, in the case of the PP/PMMA-L with shear at 50 s^{-1}, the onset temperature was around at 158 ^{o}C, which was much higher than that of PP (around at 132 ^{o}C). In the case of the PP/PMMA-M, the onset temperature was slightly higher than that of PP. On the other hand, PP/PMMA-H showed almost the same as the onset temperature with PP. This result implied that the addition of PMMA-H did not promote shear-induced crystallization.

The DLI values of PP were lower than 50%, This is due to the light scattering from the crystalline structure and spherulite texture. In the case of the blend, the light scattering from phase separate structure also generated the light scattering.

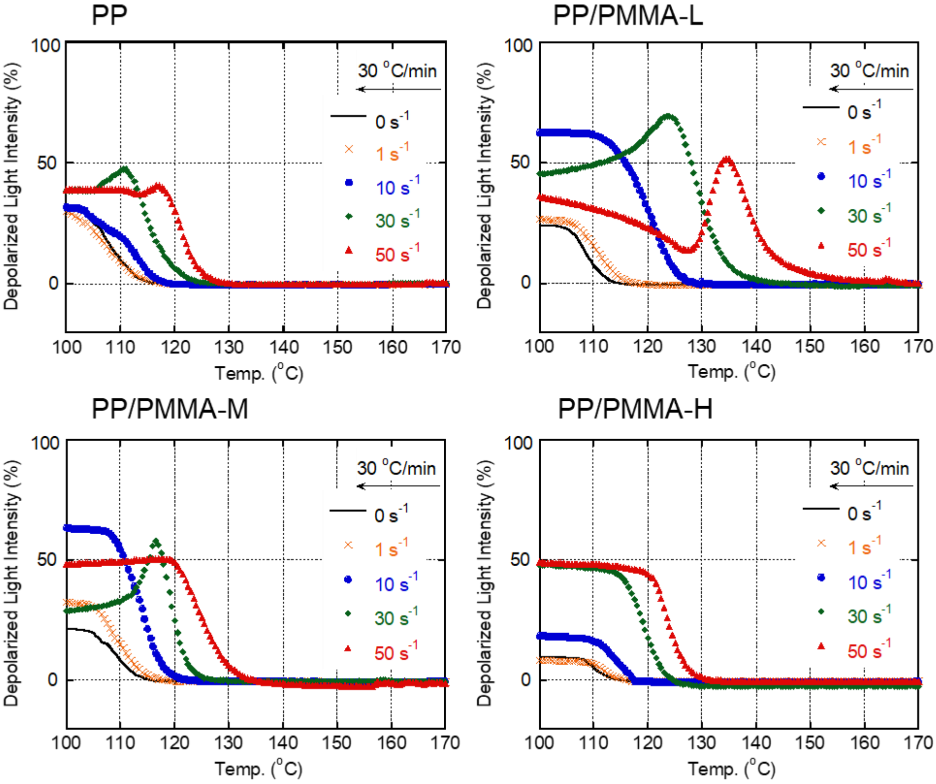

Fig. 3. Growth curves of depolarized light intensity (DLI) for PP and the blends obtained during cooling at a rate of 30 °C min^{-1}. The samples had a shear history from 190 to 160 °C at various shear rates.

Fig. 4 shows SEM images of the cut surfaces of the blend films obtained after the DLI measurements. The arrows represent the flow direction. Each film was cooled with a shear history from 190 to 160 °C at a shear rate of 50 s^{-1}. In the blend with PMMA-L, the dispersion was greatly deformed to the flow direction. The aspect ratio was very high. Because the viscosity of PMMA-L was much lower than that of PP, the droplets deformed affinely and solidified before the Rayleigh disturbance [5]. Some deformation did occur in the case of the blend with PMMA-M. In contrast, the PMMA-H particles did not show deformation. These spherical particles would rotate in a shear field as reported previously [9].

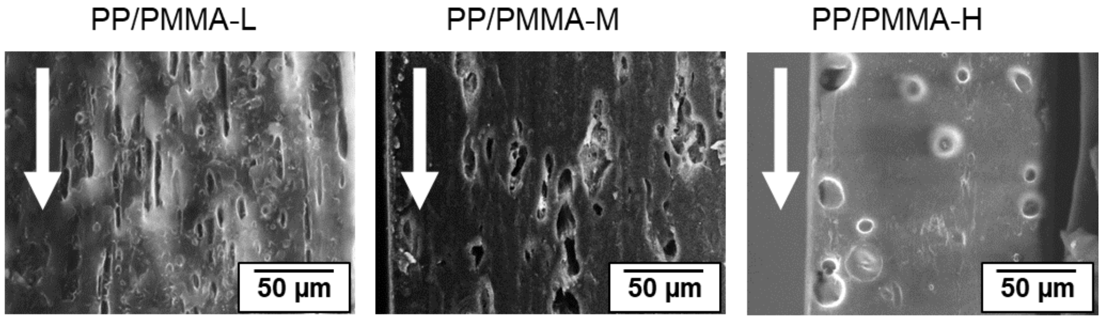

Fig. 4. SEM images of the cut surfaces of the blend films obtained after cooling. The samples had a shear history from 190 to 160 °C at 50 s^{-1}. The arrows in the pictures indicate the flow direction.

Fig. 5 shows the azimuthal angle distribution of the (110) and (040) planes. As shown in the figure, PP/PMMA-L produced sharp peaks on the equator, i.e., 90 and 270°, for the (040) diffraction plane. In the case of the (110) plane, double peaks were detected on each polar besides the peaks on equator. These were due to the tangential daughter lamellae growing from original parent lamellae developed in the perpendicular to the flow direction. These results demonstrated that adding PMMA-L enhanced the molecular chain orientation of PP. On the other hand, the addition of PMMA-M and PMMA-H barely enhanced the chain orientation. This result indicated that the addition of PMMA-M and PMMA-H did not promote the shear-induced crystallization.

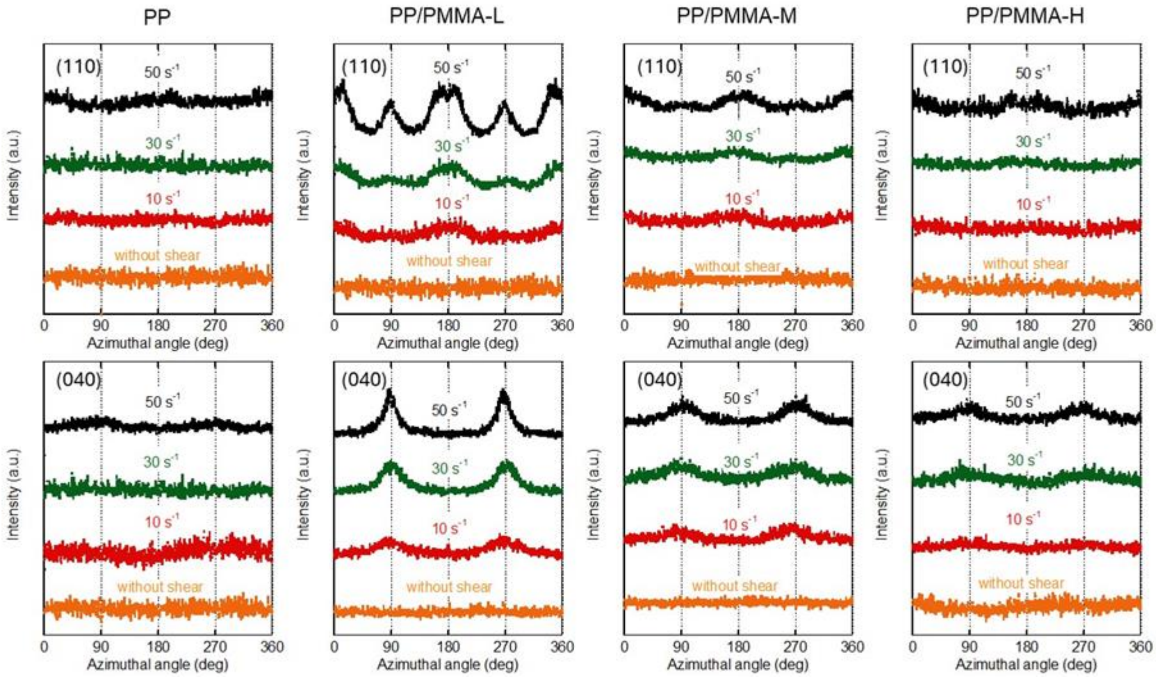

Fig. 5. Azimuthal angle distributions of the (top) (110) and (bottom) (040) planes of the α crystals in the films.

Conclusion

The addition of low-molecular-weight PMMA (PMMA-L) accelerated the shear-induced crystallization of PP. During cooling, rheological properties of PMMA-L change greatly, especially near its glass transition temperature. During cooling process with shear, PMMA-L deformed at high temperature and then it was glassified. It provided an increase in the actual shear rate of PP. As a result, Shear-induced crystallization of PP was enhanced. Because of the pronounced shear-induced crystallization, the orientation of PP chains, which causes high rigidity, was greatly enhanced. In contrast, by addition of PMMA-H, these spherical particles were considered to rotate in a shear field. As a result, PMMA-H particle disturbed PP orientation, and thus did not enhance shear induced crystallization.

Reference

[1] Z. Ma, L. Balzano, G. Portale, G.W.M. Peters, Flow induced crystallization in isotactic polypropylene during and after flow, Polymer, **55** 6140–6151 (2014).

[2] F.G. Hamad, R.H. Colby, S.T. Milner, Onset of flow-induced crystallization kinetics of highly isotactic polypropylene, Macromolecules, **48** 3725–3738 (2015).

[3] J.M. Dealy, D.J. Read, R.G. Larson, Structure and Rheology of Molten Polymers, second ed., Hanser, Munich, 2005.

[4] L.J. Fetters, D.J. Lohse, W.W. Graessley, Chain dimensions and entanglement spacings in dense macromolecular systems, J. Polym. Sci., Part B: Polym. Phys., **37** 1023–1033 (1999).

[5] H.E.H. Meijer, J.M.H. Janssen, P.D. Anderson, Mixing of immiscible liquids, in Mixing and compounding of polymers, theory and practice, in: I. Manas-Zloczower Ed., Mixing and Compounding of Polymers, second ed., Hanser, Munich, Chap.4, 2009.

[6] G.K. Batchelor, Slender-body theory for particles of arbitrary cross-section in Stokes flow, J. Fluid Mech., **44** 419–440 (1970).

[7] G.K. Batchelor, The stress generated in a non-dilute suspension of elongated particles by pure straining motion, J. Fluid Mech., **46** 813–829 (1971).

[8] J.D. Goddard, Tensile stress contribution of flow-oriented slender particles in non Newtonian fluids, J. Non-Newtonian Fluid Mech., **1** 1–17 (1976).

[9] H. Zhou, Y.F. Zhang, Effect of aromatic dihydrazide compounds on crystallization behavior and mechanical properties of isotactic polypropylene, J. Therm. Anal. Calorim., **147** 6239–6247 (2022).